551.521.3 (- 061.1.80°)

Radiative equilibrium temperature of the atmosphere along 80°E longitude

R. V. GODBOLE, R. R. KELKAR and T. MURAKAMI*

Institute of Tropical Meteorology, Poona

(*Received 5 June 1969*)

ABSTRACT. Radiative equilibrium temperature has been computed as the asymptotic steady state of an initial value problem by marching process. The sigma-coordinate system has been used in which the earth's surface is one of the coordinate surfaces. The effects of long wave radiation due to water vapour, carbon dioxide, and ozone and of absorption of solar radiation by these gases have been taken into account. Also, the effects of reflected solar energy by clouds have been considered and the scheme developed in this regard has been described.

The heat balance condition at the earth's surface has been used to predict the surface temperature. The effect of convection has been included such that the computed lapse rate is adjusted to dry adiabatic lapse rate whenever the lapse rate exceeds the dry adiabatic lapse rate.

The results show that ozone is mainly responsible for maintaining warm stratosphere and that in the stratosphere the conditions of radiative equilibrium are satisfied. In the troposphere, there is a net radiative cooling. The equilibrium solution also reveals tropopause height variation with latitude.

1. Introduction

Radiation is the primary source of energy that drives the general circulation of the atmosphere. Studies on the general circulation, therefore, must define precisely the distribution of radiative heat sources and sinks. In order to describe the heat sources and sinks over any region, it is necessary to know the radiative temperature changes due to the incoming solar radiation and the outgoing terrestrial radiation. If we consider the atmosphere to be horizontally stratified, then at any level in it, there is a certain amount of radiative heat in the upward as well as the downward direction. There must, therefore, exist a temperature at any level which is in equilibrium with the two opposing radiative heat fluxes. The value of this temperature which is known as the radiative equilibrium temperature may be obtained as the asymptotic solution by marching process from certain initial condition. An attempt is made, in the present work, to determine the radiative heat sources and sinks by actually applying the equations of radiative heat transfer.

2. Computational Scheme

Absorption of direct and reflected solar radiation by water vapour, carbon dioxide, and ozone as well as the effects of long wave radiation due to these three gases have been considered. The distributions of the absorbing gases are determined from observations, using the available data for the period chosen. Albedo at the earth's surface has been determined empirically by considering the cloud amount, the precipitation and the surface conditions during the monsoon season.

Coordinate system — The radiative equilibrium temperature has been computed for a monsoon month of July 1964-65 and along 80°E from equator to north pole at a five-degree-latitude interval. This choice offers a variety of surface features, *viz.*, ocean, land, mountain, and ice. In Fig. 1(a), the grid point 1 is located at half the grid distance outside the equator and the grid point 20 is similarly located outside the north pole. In the vertical, the sigma coordinate is used in which the pressure is normalized by the surface pressure, *i.e.*, $\sigma = p/p_*$, p_* being the surface pressure (For details *see* Appendix). Fig. 1(b) shows the various σ levels into which the atmosphere from the surface upto the top has been divided, and Fig. 2 demonstrates their latitudinal dependence and heights. This system has been used so as to facilitate incorporation of the effects due to radiation, as will be computed here, directly into a broad-based monsoon model which has been developed for the study of the monsoon circulation.

*Present affiliation : Department of Geosciences, Univertsity of Hawaii, Honolulu, U.S.A.

Flux of infra red radiation and cooling — Following Manabe and Möller (1961), the expressions for the downward (D_σ) and upward (U_σ) flux of radiation at any reference level σ due to water vapour are written as (*see* Appendix also for the finite difference scheme used)—

$$D_\sigma = \pi B_c \bar{\epsilon}_f (y_o, T_c) - \int_{B_0}^{B_c} \bar{a}_f (y_o, T) \pi \, dB - \int_{B_\sigma}^{B_0} \bar{a}_f (y, T) \pi \, dB \quad (1)$$

$$U_\sigma = \pi B_* - \int_{B_\sigma}^{B_*} \bar{a}_f (y, T) \pi \, dB \quad (2)$$

and for carbon dioxide and ozone are written as

$$D_\sigma \simeq \pi b_o \bar{A}_f (y_o, T) - \int_{b\sigma}^{b_o} \bar{A}_f (y, T) \pi \, db \quad (3)$$

$$U_\sigma \simeq \pi b_* - \int_{b_\sigma}^{b^*} \bar{A}_f (y, T) \pi \, db \quad (4)$$

Here, B_c, B_0, B_σ and B_* are the black body fluxes at temperatures T_c, T_0, T_σ and T_* respectively in the case of water vapour absorption bands and b_o, b_σ and b_* are the black body fluxes at temperatures T_o, T_σ and T_* respectively in the case of carbon dioxide and ozone absorption bands. T_c is the temperature introduced for convenience of integration. The subscript ($_*$) refers to the earth's surface.

$$y_o = | u_\sigma - u_o |, \quad y = | u_\sigma - u |$$

where u_σ is the optical depth measured from the top of the atmosphere to the level σ. $\bar{\epsilon}_f (y, T)$, and $\bar{a}_f (y, T)$ are the mean slab emissivity and the mean slab absorptivity respectively for water vapour and $\bar{A}_f (y, T)$ is the mean slab absorptivity for carbon dioxide or ozone.

The optical depth for any absorbing gas in a layer of thickness $\Delta\sigma$ is obtained by

$$\Delta u = \frac{p_*}{g} \left(\frac{\sigma p_*}{p_0} \right)^k r \, \Delta\sigma \quad (5)$$

where r is the mixing ratio of the gas and p_o = 1000 mb; and $(\sigma p_* / p_0)^k$ is the pressure correction factor. The values of k for water vapour, carbon dioxide, and ozone are 0·6, 0·86 and 0·3 respectively (Manabe *et. al* 1961).

The cooling at any level σ is given by

$$\frac{\partial T_\sigma}{\partial t}\Big)_{LR} = \frac{g}{c_p} \frac{1}{p_*} \frac{\partial F_\sigma}{\partial \sigma} \quad (6)$$

where the subscript *LR* stands for the long wave radiation. F_σ represents the net flux which is the difference between the upward flux (U_σ) and downward flux (D_σ) defined in equations (1) through (4). In practice, the long wave radiational coolings is computed separately for the three gases, so that—

$$\frac{\partial T}{\partial t}\Big)_{LR}^{\text{Total}} = \frac{\partial T}{\partial t}\Big)_{LR}^{W} + \frac{\partial T}{\partial t}\Big)_{LR}^{C} + \frac{\partial T}{\partial t}\Big)_{LR}^{o} \quad (7)$$

Flux of solar radiation and heating — The heating due to the absorption of solar radiation may be separated into two components as

$$\frac{\partial T}{\partial t}\Big)_{SR} = \frac{\partial T}{\partial t}\Big)_{SR}^{D} + \frac{\partial T}{\partial t}\Big)_{SR}^{R} \quad (8)$$

where the first term with superscript D represents absorption of direct solar radiation and the second term with superscript R represents the abosorption of reflected diffused solar radiation. Subscript *SR* stands for the solar radiation.

The daily mean rate of temperature change due to direct solar radiation is given by —

$$\frac{\partial T_\sigma}{\partial t}\Big)_{SR}^{D} \simeq \frac{\text{daytime}}{\text{whole day}} \frac{g}{c_p} \frac{\cos \bar{\xi}}{p_*} \times \frac{\partial}{\partial \sigma} a \, (y_o \sec \bar{\xi}) \quad (9)$$

where $\bar{\xi}$ is the mean zenith distance of the sun during the daytime.

The heating due to reflected solar radiation for any gas is given by —

$$\frac{\partial T_\sigma}{\partial t}\Big)_{SR}^{R} = - \frac{g}{c_p} \frac{R_e}{S} \frac{\partial}{\partial \sigma} a \, (1{\cdot}66 \, y_*) \quad (10)$$

where y_* is the optical depth measured from the bottom of the atmosphere upto the level σ.

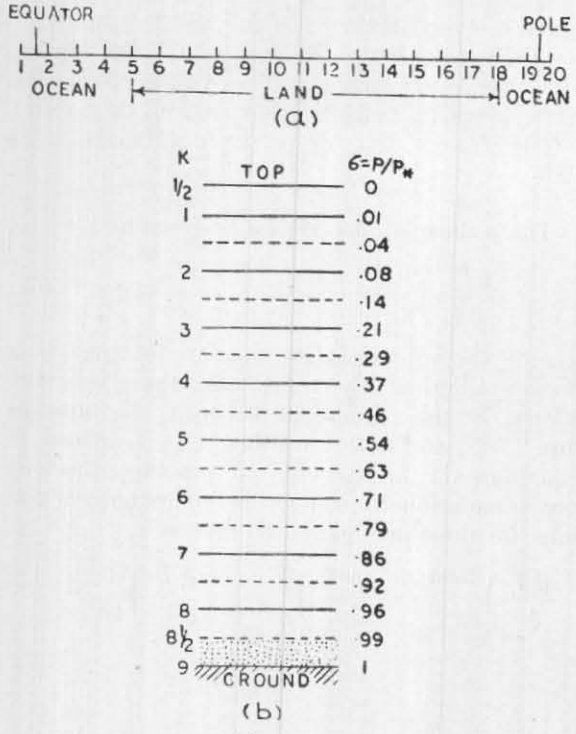

Fig. 1

(a) Horizontal grid in N-S, the grid internal being 5° Lat.

(b) Various sigma-levels in the vertical from the gound up to the top of the atmosphere

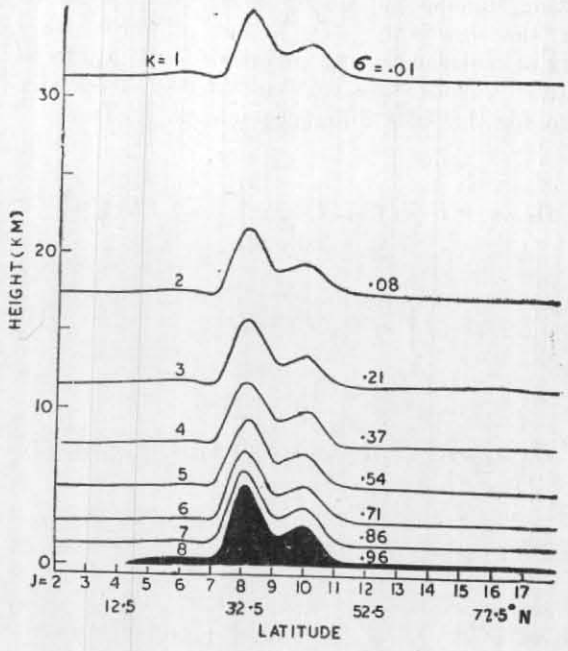

Fig. 2. Latitudinal variation of the height of the sigma-level

According to Elsasser *et. al* (1960), the effective optical depth for reflected diffused radiation is 1·66 times that for direct solar radiation. S denotes the solar constant (2 cal/cm^2 /min) and R_e the reflected solar radiation.

In estimating R_e it may be separated into two components as —

$$R_e = R_g + R_c$$

where R_g and R_e represent reflected radiation from the ground and cloud respectively. R_g may be written as —

$$R_g \simeq \frac{\text{daytime}}{\text{whole day}} \cos \bar{\xi}\ \alpha_* [S - -a^T (y_{o,*} \sec \bar{\xi})] \qquad (11)$$

where α_* is the surface albedo. $y_{o,*}$ is the optical depth from the top to the bottom of the atmosphere, and

$$a^T (y_{o,*} \sec \bar{\xi}) = a^W (y_{o,*} \sec \bar{\xi}) + a^C (y_{o,*} \sec \bar{\xi}) + a^0 (y_{0,*} \sec \bar{\xi}) \qquad (12)$$

Let α_1 (= 0·2), α_2 (= 0·5), and α_3 (= 0·7) be reflectivities and n_H, n_M, and n_L be the amounts of high, medium, and low clouds respectively (Manabe and Strickler 1964). In Fig. 3 is shown the amount of reflection at the top of each type of cloud. The total reflectivity of the clouds is given by

$$RS_* = [\alpha_1 n_H + \alpha_2 (1 - \alpha_1 n_H) n_M + \alpha_3 (1 - \alpha_1 n_H)(1 - \alpha_2 n_M) n_L] \qquad (13)$$

and the amount of solar energy reflected by these clouds is given by —

$$R_c \simeq \frac{\text{daytime}}{\text{whole day}} \cos \bar{\xi}\ S (R S_*) \qquad (14)$$

Since the energy R_c does not contribute to heat the earth's surface, we assume, for simplicity, that R_c is the solar energy reflected from the earth's surface itself. Combining (11) and (14), the total reflection R_e is given by —

$$R_e \simeq \frac{\text{daytime}}{\text{whole day}} \cos \bar{\xi}\ \alpha_{*e} [S - -a^T (y_{0,*} \sec \bar{\xi})] \qquad (15)$$

where α_{*e} is the effective albedo defined by

$$\alpha_{*e} = \alpha_* + \frac{RS_*}{1-a^T\ (y_{0,*}\ \sec\ \overline{\xi}\ )\ /\ S}\ ,$$

$$0 \leqslant \alpha_{*e} \leqslant 1 \qquad (16)$$

The net solar radiation absorbed by the earth's surface is —

$$S_* \simeq \frac{\text{daytime}}{\text{whole day}}\ \cos\overline{\xi}\ (1-\alpha_{*e})\ [S - -a^T\ (y_{o,*}\sec\overline{\xi})\ ] \qquad (17)$$

Sea surface temperature — Since the temperature of the sea remains sensibly constant with respect to time, the sea is assumed to have infinite heat capacity. The sea surface temperature has, therefore, been fixed at the observed mean value.

Ground temperature — Over the land, the temerature at the earth's surface is not constant with respect to time and hence it is predicted by applying heat balance condition at the earth's surface. Heat balance should exist between the net downward solar radiation, the downward long wave radiation, the upward long wave radiation, and the sensible and latent heat fluxes at the earth-atmosphere interface.

Convective adjustment — Pure radiative processes operating alone would give rise to superadiabatic lapse rate in the lower troposphere (Manabe and Möller 1961). This means that other dynamical processes, mainly the convective processes, control the temperature distribution of the lower atmosphere. The effect of convection has been incorporated. The procedure adopted is the one used by Smagorinsky *et al.* (1965), in which the computed lapse rate is adjusted to dry adiabatic lapse rate whenever the lapse rate, in course of marching process, exceeds the dry adiabatic lapse rate. In other words, the temperature lapse rate at any time step is not allowed to exceed the dry adiabatic lapse rate (*see* Appendix for details). This procedure of convective adjustment will transfer heat from the earth's surface into the lower and upper troposphere.

Boundary conditions — At the top of the atmosphere, the downward long wave radiation is assumed to be zero. A value of 2 cal/cm^2/min has been adopted for the solar constant.

The temperature at the earth's surface has been determined such that it satisfies the requirement of heat balance. If the heat capacity of the earth is assumed to be zero, the balance equation may be written as

$$S_* + (DLR)_* = s\,T_*^4 - c_p\,T_*^Z - L\,\mu_*^Z \qquad (18)$$

where the subscript ($_*$) stands for the quantities at the earth's surface. S_* and $(DLR)_*$ are the net downward solar radiation and the downward long wave radiation respectively at the earth's surface. s is the Stafan-Boltzman constant. $c_p\,T_*^Z$ and $L\mu_*^Z$ represent the upward sensible and latent heat exchange respectively at the earth-atmosphere interface which are ultimately functions of surface wind and the temperature gradient across the earth's surface (for details *see* Appendix and also refer Murakami *et. al*† 1968).

Computation of radiative equilibrium temperature — The basic principle is to approach the state of radiative equilibrium asymptotically from certain initial condition. The forward time difference scheme with the interval of time $\triangle t$ as six hours was adopted throughout the computations. The prediction equation may be written as —

$$T\ (Z, t+\triangle t) = T\ (Z, t) + \frac{\partial\, T\ (Z,T)}{\partial\ t}\triangle t \qquad (19)$$

Equilibrium was considered to have been reached when the difference between the daily mean temperatures of two consecutive days was less than 0·01 deg. (The daily mean temperature is defined as the average temperature over four successive time steps).

3. Basic Data

Water vapour — The distribution of the absorbing gases is determined from observations along 80°E, supplemented by available information at different longitudes.

The mixing ratio of water vapour has been determined by using *Daily Weather Map with Synoptic Data Tabulation* of the Japan Met. Agency and the *Daily Series, Northern Hemispheric Data Tabulations* of the U.S. Weather Bureau for July 1964–65. Analysis of the mixing ratio at standard isobaric levels has been made and the values were read at each grid point along 80°E. These were further plotted individually as height-temperature profiles. Mixing ratio

† Numerical Experiment of the monsoon along 80° E longitude by Murakami, T., Godbole, R.V. and Kelkar, R.R., ITM, Sci. Rep. No. 63, 1968.

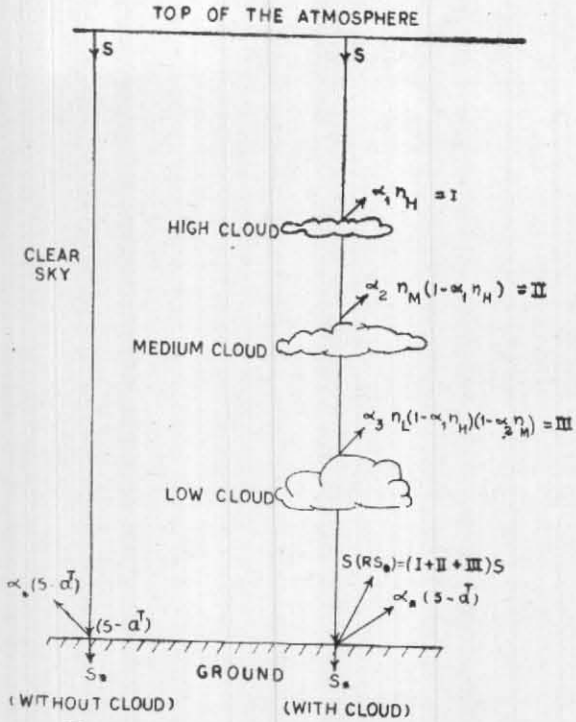

Fig. 3. Passage of solar radiation through the atmosphere with and without clouds
Absorption inside the clouds is neglected

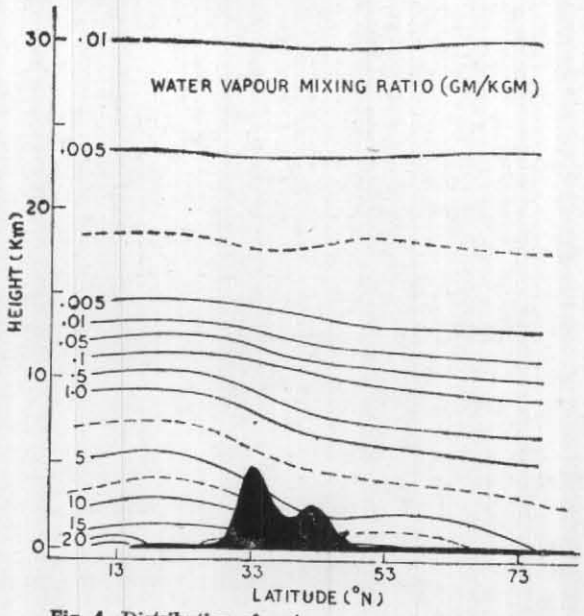

Fig. 4. Distribution of water vapour as a function of latitude and height

above 500 mb was extrapolated until a line of constant frost point of 190° K is reached. Thereafter the mixing ratio was assumed to follow constant frost point of 190° K irrespective of latitude upto a height of 30 km, as considered by Manabe and Möller (1961). Above 30 km, a constant mixing ratio line has been followed.

At the earth's surface, the mixing ratio of water vapour has been determined by using the relation —

$$r_* = \beta\, r_s\,(T_*) \qquad (20)$$

where r_* is the mixing ratio at the earth's surface. β is the constant arbitrarily fixed and $r_s\,(T_*)$ is the saturation mixing ratio at the surface temperature T_* . β is considered to be unity for the sea surface. It is assumed to be 0·8 for the land and 0·6 for the mountain. The distribution of water vapour, thus determined, is presented in Fig. 4.

Carbon dioxide — The mixing ratio of carbon dioxide has been assumed to be constant at 0·456 (gm/kgm) for all the levels and for all the latitudes.

Ozone — The ozone mixing ratio has been determined on the basis of the *Ozone Data of the World* published by the Canadian Met. Service and the cross-sections published earlier by Ramanathan and Kulkarni (1961); and Murgatroyd (1964). In Fig. 5, is shown the ozone distribution with respect to height and latitude.

Albedo — The values of surface albedo as given by the *Smithsonian Tables* for different surface conditions have been adopted.

Cloud — The cloud amount has been determined from the *Daily Weather Map with Synoptic Data Tabulation* of Japan Met. Agency and the *Daily Series, Northern Hemispheric Data Tabulations* of the U.S. Weather Bureau for July 1964-65.

Absorptivity and emissivity — The values of mean slab absorptivity and emissivity for water vapour, carbon dioxide, and ozone and also those of solar radiation by these gases have been used as given by Manabe and Möller (1961).

4. Results and Discussion

Fig. 6 shows how the equilibrium temperature distribution is being approached from an initial condition of isothermal atmosphere at 305°K. It is seen that final equilibrium is reached after 225 days which is equivalent to 900 time steps. As computations commence from zero time, the intitial condition of isothermalcy is quickly disturbed. Below 18 km, the tropospheric and lower stratospheric characteristics

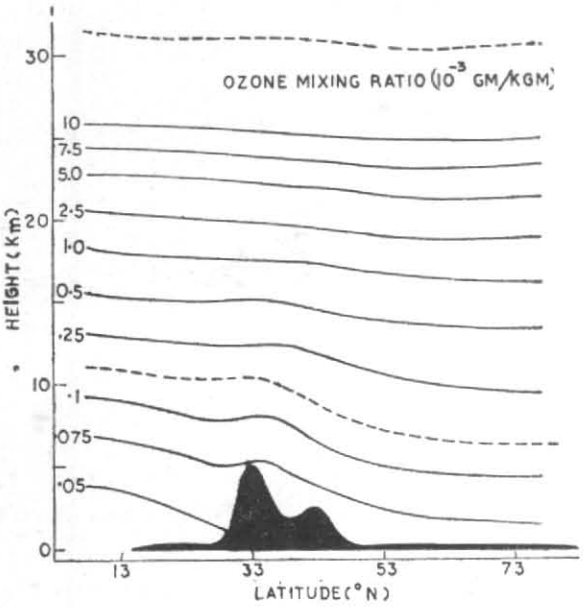

Fig. 5. Distribution of ozone as a function of latitude and height

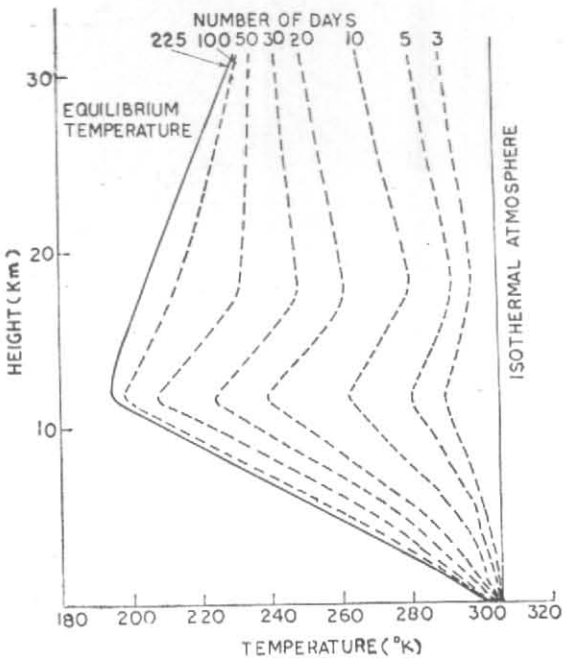

Fig. 6. Approach to radiative equilibrium temperature with convective adjustment from an initial condition of isothermal atmosphere at 305°K

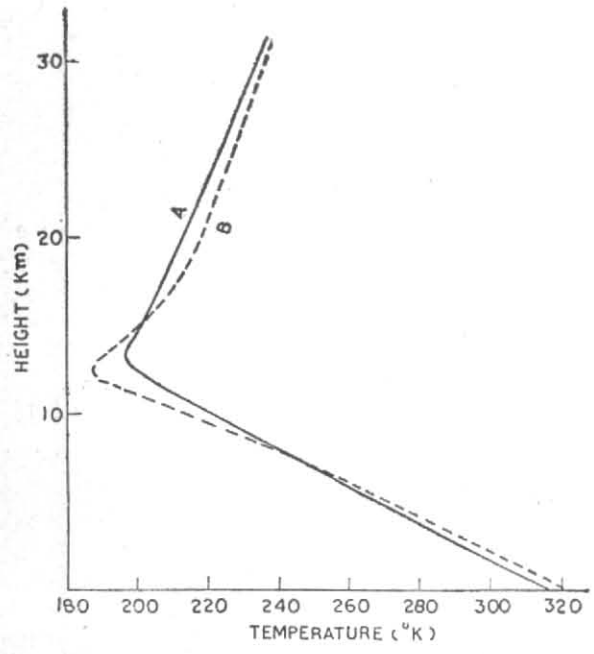

Fig. 7. Radiative equilibrium temperature

(A) with convective adjustment and
(B) without convective adjustment

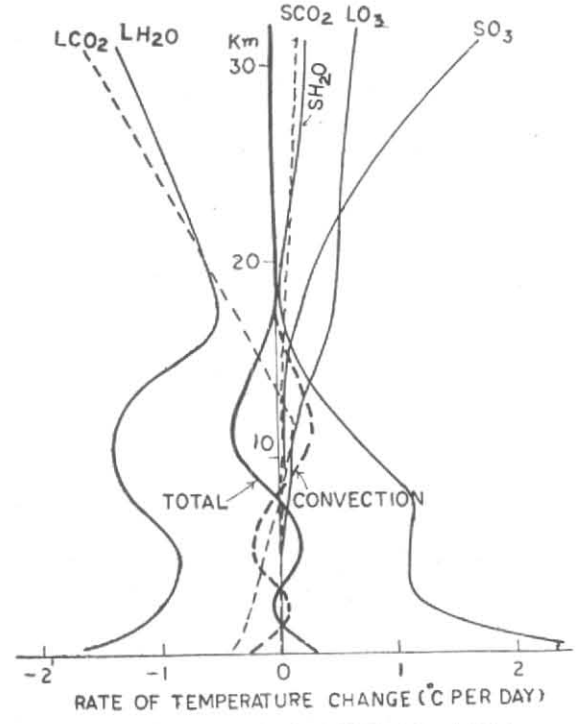

Fig. 8. Cooling and warming (°C/day) due to Water vapour (H_2O), Carbon dioxide (CO_2), and Ozone (O_3).

LH_2O, LCO_2 and LO_3 represent the temperature change due to long wave radiation. Solid full line represent the total cooling and warming; solid broken line the effects of convection

of temperature profile begin to develop and these are maintained progressively in the right direction. This, however, is not the case for the stratospheric region above 18 km, wherein the temperature decreases at first with height upto about 50 days and thereafter changes sign. It then progressively attains the observed stratospheric temperature characteristics. It is also seen from the figure that, to start with, the daily temperature variations are very large. As the iterations continue, the temperature variations between consecutive time steps become smaller and smaller until they practically vanish, *i.e.*, become less than a small value δ which has already been prescribed.

The results of Fig. 6 are for latitude 22·5°N. In the computations, the temperature at the earth's surface is not predicted but is fixed at 305°K which is the observed temperature at 22·5°N for July. The procedure of convective adjustment at each time step has been incorporated.

In Fig. 7, which also refers to 22·5°N, curves A and B show the radiative equilibrium temperature profiles with and without convective adjustment respectively. In both the cases, the surface temperature has been predicted by the use of equation (18). It is seen that the predicted surface temperature with convection (317°K, curve A) is less than that without convection (320°K, curve B). This means that energy equivalent to the difference between the two temperatures has been transported upward by convection.

The predicted surface temperatures in both the curves A and B are rather high as compared to what is observed (305°K). The difference could be partly due to the neglect of conduction of heat into the ground and that of energy transport in the zonal and meridional directions at the earth's surface.

The radiative heating and cooling components individually due to water vapour, carbon dioxide and ozone are plotted in terms of rate of temperature change in Fig. 8. The results correspond to those obtained in the final time step with no convective adjustment having been made. It is seen that in the lower layers, the contribution of water vapour to infra-red cooling (LH_2O) as well as solar heating (SH_2O) is very large compared to those of carbon dioxide (LCO_2, SCO_2) and ozone (LO_3, SO_3). Near the ground, both the cooling (1·7°C per day) and the heating (2·4°C per day) are maximum.

In the upper layers, the conspicuous feature noticed is the rapid increase with height of heating

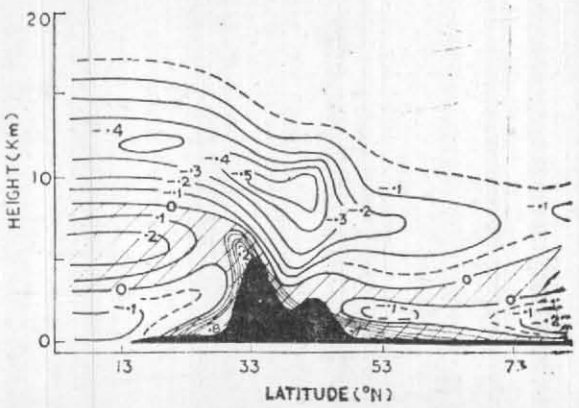

Fig. 9. Vertical cross-section of warming and cooling due to solar and infra-red radiation

(SO_3) due to the absorption of solar radiation by ozone. Ozone, by virtue of its distribution in the vertical, contributes to the heating in the infra-red (LO_3) also. Thus, ozone is seen to be mainly responsible in maintaining warm stratosphere.

The total effect of the individual radiative heating and cooling components is also shown in Fig. 8. There is practically no net temperature change above 17 km which means that the conditions of radiative equilibrium are satisfied in the stratosphere. In the troposphere, however, there is a net radiative cooling indicating that the troposphere is not in radiative equilibrium and the effect of convection has, therefore, to be taken into account in order to arrive at an equilibrium (no net temperature change) state. That this has been the case is clearly seen in the figure in which the rate of temperature change obtained by convective adjustment in the final time step has also been plotted.

The total heating and cooling due only to radiation for all the latitudes from equator to north pole is shown in Fig. 9. Except in the region of Indian Ocean, there is a large heating near the earth's surface. It is maximum (2°C per day) over the Himalayas. This is because, firstly, the incoming solar radiation is maximum at about 35°N in July and secondly, the albedo considered for the Himalayas (0·6) is higher than that for the sea surface (0·05) and for land (0·2). Higher albedo causes a large amount of reflected solar energy available for absorption again. There is a belt of warming at about 5 km and cooling above. In the stratosphere, as is expected, there is no net cooling or warming due to radiation.

One interesting feature brought out is that the compensation required due to convective adjustment should be maximum over the Himalayas entailing a higher degree of convective activity

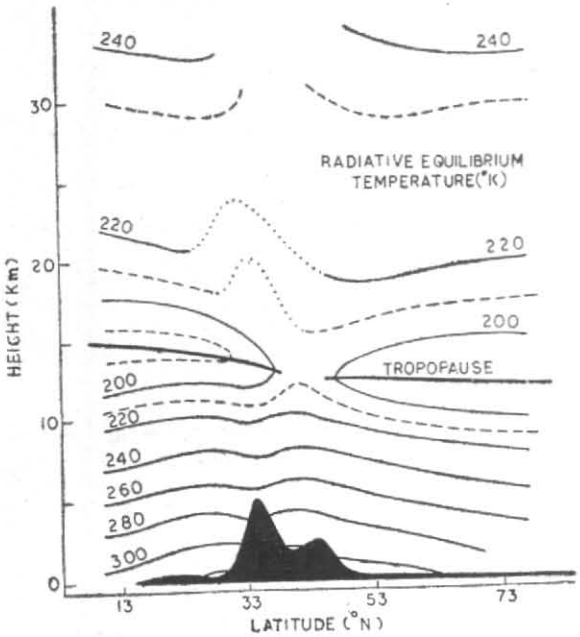

Fig. 10. Radiative equilibrium temperature with convective adjustment as a function of latitude and height

The dotted portion of the isotherms denotes their ambiguous nature

over the region. The inference which is to be confirmed by observation is only indirect and is subject to the limitation that the horizontal transport of heat has been disregarded.

The vertical cross-section of the temperature along 80°E from equator to north pole is shown in Fig. 10. It is seen that the presence of the Himalayas distorts the temperature field. The maximum temperature (325°K) occurs at the southern foot of the Himalayas. There is a feeble temperature dip over the Himalayas although the heating there has been maximum (Fig. 9). The main reason for the appearance of the dip is that the albedo considered for the Himalayas being high, the black body emission from the ground is reduced and this consequently maintains the low temperature at higher levels too. The higher albedo for the Himalayas also accounts for the prominent ridge as noticed in the stratosphere (indicated by the dotted lines). Ozone at that height obtains more amount of reflected solar energy for absorption on account of higher albedo considered for the region.

The decrease of tropopause height with latitude is clearly discernible in Fig. 10, especially south of the Himalayas which is in contrast with the result of Manabe and Möller who found practically no variation of tropopause height with latitude for July (Fig. 18 of Manabe and Möller 1961). The computed height of the tropopause over the equator is 14 km which is less than the normally observed height of about 17 km. Over the pole, the computed tropopause height is 11 km which is close to what is observed in July. The features suggest that the dynamical processes are more active over the equator than over the north pole in effecting changes in the radiative equilibrium temperature field.

The variation of tropopause height with latitude is mainly due to radiative processes. Over the equator water vapour penetrates to higher levels as compared to that over the poles (*see* Fig. 4). Ozone, on the other hand, is more over the high latitudes than over the equator (*see* Fig. 5). The net result is that the cooling effect due to water vapour penetrates to higher levels over the equatorial regions whereas the warming due to ozone begins from much lower levels upward over the polar regions.

5. Conclusion

The study has shown that temperature equilibrium is attained in the stratosphere by radiation. In the troposphere, in addition to radiation, other processes such as convection should play an important role in controlling the temperature distribution. The existence of warm stratosphere is due to the unique action of ozone as seen both in the infra-red and solar radiation range. The study has also brought out the profound influence of the Himalayas on the radiative heat exchange processes. Existence of strong convection has been suggested over the Himalayas in the absence of horizontal compensation of heat. Better agreement has been revealed between the calculated and observed tropopause height at higher latitudes. In the present study, the effects due to advection and condensation have not been taken into account. These will have to be incorporated for obtaining a truer picture of the heat sources and sinks in the atmosphere.

6. Acknowledgement

The authors wish to express their thanks to Dr. Bh. V. Ramana Murty for his interest in the study, for going through the manuscript and for making useful suggestions. Thanks are also due to our colleagues in the Drawing Section for preparing the diagrams and to Shri A.E. Lohokare for typing the manuscript.

REFERENCES

Elsasser, W. M. and Culbertson, M. F.	1960	*Met. Mongr.*, **23**, pp. 43.
London, J., Ohring, G. and Ruff, I.	1956	Radiative properties of the stratosphere. Final Rep., contract AF 19 (604)—1285 Res. Div., College of Engng, New York Univ., pp. 48.
Manabe, S. and Möller, F.	1961	*Mon. Weath. Rev.*, **89**, pp. 503-532.
Manabe, S. and Strickler, R. F.	1964	*J. atmos. Sci.*, **21**, pp. 361-385.
Murgatroyd, R. J.	1964	Ozone and water vapour in the upper troposphere and lower stratosphere. *Tech. Note*, 68, WMO No. 169. TP. 83, pp. 68-69.
Ramanathan, K. R. and Kulkarni, R. N.	1960	*Quart. J. R. met. Soc.*, **86**, pp. 151-155.
Smagorinsky, J., Manabe, S. and Holloway, Jr., J. L.	1965	*Mon. Weath. Rev.*, **93**, pp. 727-768.

APPENDIX

The eight reference levels in the vertical used in this study are not equally spaced with respect to σ, but are so arranged as to give maximum resolution at the extremities of the atmosphere. σ is expressed as (Smagorinsky *et al.* 1965)—

$$\sigma_k = Q_k^2 (3 - 2 Q_k) = p_k / p_* \qquad \text{(A-1)}$$

where,

$$Q_k = (2k - 1) / 17, \qquad k = \tfrac{1}{2}, 9, \tfrac{1}{2} \qquad \text{(A-2)}$$

The suffix k stands for any given level. In Table 1 are shown the values of σ, height, pressure, and temperature for various values of k.

The standard atmospheric temperature distribution in the vertical is taken as the initial temperature for all the latitudes so that no temperature gradient exists along any isobaric level. The surface pressure p_* has been estimated by interpolation from the standard atmosphere using the terrain at the grid point in question. Due to the existence of the Tibetan Plateau, p_* significantly changes with respect to latitude and hence the temperature along any σ-level will change with latitude.

Equation (1) which expresses the downward flux due to water vapour has been expressed in the finite difference form as follows—

$$D_{\frac{1}{2}} = 0 \qquad \text{(A-3)}$$

$$\begin{aligned} D_{k-\frac{1}{2}} = {} & \pi B_c [\bar{\epsilon}_f (y_o, T_c) - \overline{a_f} (y_o, T)] + \\ & + \pi B_1 [\overline{a_f} (y_o, T) - \epsilon (2) - \epsilon (3)] + \\ & + \pi \sum_{i=2}^{k-2} B_i [\epsilon (2i - 2) + \epsilon (2i - 1) - \epsilon (2i) \\ & - \epsilon (2i + 1)] + \pi B_{k-1} [\epsilon (2k - 4) + \\ & + \epsilon (2k - 3) - \epsilon (2k - 2)] + \\ & + \pi B_k \epsilon (2k - 2) \end{aligned}$$

$$k = 2, 9 \qquad \text{(A-4)}$$

TABLE 1

The sigma system in the vertical with associated values of pressure (p), height (H) and temperature (T)

k	Q	σ	p (mb)	H (km)	T (°C)
0·5	0·000	0·000	0·000	∞	—
1·0	·059	·010	10·102	31·14	—45·51
1·5	·118	·038	38·767	22·28	—54·30
2·0	·176	·082	83·522	17·37	—56·50
2·5	·235	·140	141·89	13·99	—56·50
3·0	·294	·209	211·40	11·45	—56·50
3·5	·353	·286	289·57	9·414	—46·10
4·0	·412	·369	373·91	7·668	—34·78
4·5	·471	·456	461·97	6·159	—24·99
5·0	·529	·544	551·26	4·852	—16·551
5·5	·588	·631	639·32	3·721	—9·173
6·0	·647	·714	723·69	2·751	—2·875
6·5	·706	·791	801·86	1·932	2·449
7·0	·765	·860	871·36	1·254	6·849
7·5	·824	·918	929·72	0·720	10·326
8·0	·882	·962	974·47	0·328	12·868
8·5	·941	·990	1003·15	0·085	14·447
9·0	1·000	1·000	1013·25	0·000	15·000

where the quantity ϵ is defined as —

$$\epsilon(1) = 0{\cdot}0$$
$$\epsilon(n) = \frac{0{\cdot}5}{y_n - y_{n+1}} \int_{y_{n+1}}^{y_n} \overline{a_f}\,(y, T)\, dy$$
$$n = 2, 2(k-1) \qquad \text{(A-5)}$$

Here, y_n is the optical depth between the levels $k - \frac{1}{2}$ and the level n.

To compute $\epsilon(n)$, mixing ratio of water vapour at all the 18 levels ($k = \frac{1}{2}, 9, \frac{1}{2}$) has been used. The reason for doing this is the highly non-linear change of $\overline{a_f}(y, T)$ with respect to optical depth when it approaches zero.

The downward flux at the earth's surface has been expressed as —

$$(DLR)_* = \pi B_c [\overline{\epsilon_f}(y_o, T_c) - \overline{a_f}(y_o, T)] + \pi B_1 [\overline{a_f}(y_o, T) - \epsilon(2) - \epsilon(3)] + \pi \sum_{i=2}^{8} B_i [\epsilon(2i-2) + \epsilon(2i-1) - \epsilon(2i) - \epsilon(2i+1)] + \pi B_* [\epsilon(16) + \epsilon(17)] \qquad \text{(A-6)}$$

Likewise, the upward flux defined in equation (2) is expressed as—

$$U_{k-\frac{1}{2}} = \pi B_* + \pi B_{k-1}\ \epsilon(2k-1) + \pi B_k [\epsilon(2k+1) + \epsilon(2k) - \epsilon(2k-1)] + \pi \sum_{i=k+1}^{8} B_i [\epsilon(2i+1) + \epsilon(2i) - \epsilon(2i-1) - \epsilon(2i-2)] - \pi B_* [\epsilon(17) + \epsilon(16)]$$
$$k = 1, 9 \qquad \text{(A-7)}$$

where,

$$\epsilon(n) = \frac{0{\cdot}5}{y_{n+1} - y_n} \int_{y_n}^{y_{n+1}} \overline{a_f}\,(y, T)\, dy$$
$$n = 2k - 1, 17 \qquad \text{(A-8)}$$

The heat balance condition defined by equation (18) may be expressed as —

$$S_* + (DLR)_* = sT_*^4 + c_p \rho_* k_0^2 m^2 U_* [T_* - T(8) + \frac{L}{c_p}(r_* - r(8))] \qquad \text{(A-9)}$$

Here, c_p is the specific heat at constant pressure, ρ_* is the surface density, k_o is the Karman constant and L is the latent heat of vapourisation.

The quantity m is defined as —

$$m = \left[\ln \frac{h + Z_o}{Z_o} + \frac{\triangle Z}{h + Z_o}\right]^{-1} \qquad \text{(A-10)}$$

where h denotes the thickness of the turbulence layer (85 m), Z_0 is the roughness parameter (=0·1 cm over the sea, 1 cm over the land and 10 cm over the mountain). $\triangle Z$ is the height difference between the levels 8 and $8\frac{1}{2}$. The quantity U_* in equation (A-9) is defined as

$$U_* = \sqrt{(u_*^2 + v_*^2)} \qquad \text{(A-11)}$$

where u_* and v_* are the zonal and meridional wind components respectively at the surface.

Equation (A-9) is a complicated function of T_* and hence the direct evaluation of T_* from equation (A-9) is very difficult. As such, T_* at time step ν (to be determined) is assumed as the sum of T_* at time step $\nu-1$ and a correction $\triangle T$. Thus,

$$T_{*\nu} = T_{*\nu-1} + \triangle T \qquad \text{(A-12)}$$

and $T^4{}_{*\nu}$ is approximated as —

$$T^4{}_{*\nu} \simeq T^4{}_{*\upsilon-1} + 4T^3{}_{*\upsilon-1}\, \triangle T \qquad \text{(A-13)}$$

with these assumptions, the heat balance equation in terms of the change in surface temperature is expressed as —

$$\triangle T = \frac{S_* + (DLR)_* - sT^4{}_{*\upsilon-1} - c_p \rho_* k_0^2 m^2 U_* [T_{*\upsilon-1} - T(8)]}{4T^3{}_{*\upsilon-1} + c_p \rho_* k^2{}_0 m^2 U_*} \qquad \text{(A-14)}$$

In equation (A-14), the effect of the diffusion of moisture from the ground is neglected.

The convective adjustment is made such that the computed lapse rate does not exceed the dry adiabatic lapse rate. The required temperature change δT is obtained by the following two conditions :

$$\frac{\partial}{\partial \sigma}\theta(T + \partial T, \sigma) = 0 \qquad \text{(A-15)}$$

$$\frac{c_p}{g} p_* \int_{\sigma_T}^{\sigma_B} \partial T\, d\sigma = 0 \qquad \text{(A-16)}$$

where θ is the potential temperature, and σ_T and σ_B denote the top and bottom of the unstable layer respectively. The first condition ensures the existence of dry adiabatic lapse rate while the second condition implies that the total potential energy of the atmosphere remains invariant, *i.e.*, the kinetic energy created by convection is converted into heat instantaneously.